Climate Change Impacts on Flood Risk and Asset Damages within Mapped "100 year" Floodplains of the Contiguous United States

Cameron Wobus[1], Ethan Gutmann[2], Russell Jones[1], Matthew Rissing[1], Naoki Mizukami[2], Mark Lorie[1], Hardee Mahoney[1], Andrew W. Wood[2], David Mills[1], Jeremy Martinich[3]

[1]Abt Associates, 1881 Ninth Street, Suite 201, Boulder, CO, 80302 USA
[2]National Center for Atmospheric Research, 3450 Mitchell Lane, Boulder, CO, 80301 USA
[3]U.S. Environmental Protection Agency, Climate Change Division, 1200 Pennsylvania Ave NW, Washington, DC, 20460 USA

Correspondence to: Cameron Wobus (Cameron_Wobus@abtassoc.com)

Abstract. A growing body of work suggests that the extreme weather events that drive inland flooding are likely to increase in frequency and magnitude in a warming climate, thus potentially increasing flood damages in the future. We use hydrologic projections based on the Coupled Model Intercomparison Project Phase 5 (CMIP5) to estimate changes in the frequency of modeled 1% annual exceedance probability (1% AEP, or "100-year") flood events at 57,116 stream reaches across the contiguous United States (CONUS). We link these flood projections to a database of assets within mapped flood hazard zones to model changes in inland flooding damages throughout the CONUS over the remainder of the 21st century. Our model generates early 21st century flood damages that reasonably approximate the range of historical observations, and trajectories of future damages that vary substantially depending on the greenhouse gas (GHG) emissions pathway. The difference in modeled flood damages between higher and lower emissions pathways approaches $4 billion per year by 2100 (in undiscounted 2014 dollars), suggesting that aggressive GHG emissions reductions could generate significant monetary benefits over the long-term in terms of reduced flood damages. Although the downscaled hydrologic data we used have been applied to flood impacts studies elsewhere, this research expands on earlier work to quantify changes in flood risk by linking future flood exposure to assets and damages at a national scale. Our approach relies on a series of simplifications that could ultimately affect damage estimates (e.g., use of statistical downscaling, reliance on a nationwide hydrologic model, and linking damage estimates only to 1% AEP floods). Although future work is needed to test the sensitivity of our results to these methodological choices, our results indicate that monetary damages from inland flooding could be significantly reduced through substantial GHG mitigation.

1 Introduction

Inland floods are among the most costly natural disasters in the United States (e.g., Pielke and Downton, 2000), with annual damages ranging from hundreds of millions to many tens of billions of dollars over the past century (Downton et al., 2005; NOAA, 2016). In 2016, inland flooding events in Louisiana and North Carolina alone caused over $10 billion of physical

damages to homes, businesses, and other assets (Fortune, 2016; LED, 2016). This follows on other recent years with extreme flooding in Michigan (2014) and Colorado (2013), and the mid-Atlantic floods caused by Superstorm Sandy in 2012 (NOAA, 2016). With each occurrence of these damaging flood events, there is renewed interest in determining whether climate change may be partially responsible for changes in the magnitude or frequency of these events (e.g., IPCC, 2012; Trenberth et al.,

5   2015). Although the science linking changes in climate extremes to human-caused warming is advancing (e.g., Trenberth et al., 2015; National Academies of Sciences, Engineering, and Medicine, 2016), there are still many challenges to attributing observed historical trends in flooding to human-caused climate change (e.g., Kundzewicz et al., 2014; Berghuijs et al., 2016). As a complement to these attribution studies, forward-modeling approaches using linked climate-hydrologic models could help to characterize future changes in flood risk and vulnerability (e.g., Das et al., 2013; Hirabayashi et al., 2013; Arnell and

10   Gosling, 2016).

This study evaluates 21st century flood risk and flood-related damages across the contiguous United States (CONUS) using downscaled hydrologic projections from 29 global climate models (GCMs) and 2 representative concentration pathways (RCPs) for GHG forcing. We cross-referenced spatially explicit hydrologic projections with a database of built assets within each of the mapped "100-year" floodplains in the CONUS. Using this combined dataset, we generate regional estimates of

15   how cumulative damages from what are currently 1% AEP events might change through the 21st century, due to changes in the frequency of these events through time. We then compare how flood damages might differ under a higher GHG emissions scenario (RCP 8.5) vs a lower emissions scenario (RCP 4.5). We focused on these two RCPs both for consistency with the forthcoming Fourth National Climate Assessment (USGCRP, 2015) and to help quantify changes in flood risk in response to reduced GHG emissions globally.

20   Because available hydrologic records tend to be short relative to the return interval of extreme flood events, simply detecting trends in historical flooding can be challenging (e.g., Hirsch and Ryberg, 2012; Mallakpour and Villarini, 2015; Archfield et al., 2016). Furthermore, even where hydrologic changes can be detected, concurrent changes in land use and population make it difficult to attribute changing flood damages to climate change (e.g., Pielke and Downton, 2000; Kundzewicz et al., 2014; Liu et al., 2015). Thus, there may be some advantages to using forward modeling approaches where the effects of climate

25   change can be modeled in isolation. Unfortunately, this is expensive computationally: at present the most widely used strategy for assessing changes in future flood risk requires downscaling GCM outputs to hydrologically relevant spatial scales; estimating precipitation, infiltration, and runoff within a hydrologic modeling framework; and routing the resulting flows through a model river network (e.g., Reclamation, 2014). Although less computationally demanding, studies attempting to link projected changes in extreme precipitation directly to changes in flooding (i.e., without a spatially explicit hydrologic model)

30   tend to have high uncertainties (e.g., Kundzewicz et al., 2014; Wobus et al., 2014).

Recently, computational power has increased to the point that studies using downscaled and routed GCM-derived precipitation have become more common (e.g., Gosling et al., 2010; Hirabayashi et al., 2008; Reclamation, 2014). These outputs have been used to project future flood risk at scales ranging from local (e.g., Das et al., 2013) to global (e.g., Hirabayashi et al., 2013;

Arnell and Gosling, 2016). However, to our knowledge there has not yet been a CONUS-scale assessment of how changing inland flood hydrology could translate into changing monetary damages.

2 Methods

We used simulated daily hydrographs at 57,116 stream reaches across the CONUS between 2000 and 2100 to calculate a CMIP5 modeled baseline ("current climate") 1% AEP event, and changes in the frequency of flows exceeding this magnitude through the 21st century. We quantified asset exposure and expected flood damage within mapped floodplains using a combination of Federal Emergency Management Agency (FEMA) flood maps, US Census block data, and land cover data. Because only the "100-year" floodplains are consistently mapped and available at a national scale, our model of flood damages is driven only by changes in the frequency of what are currently 1% AEP events through the 21st century. We also do not project changes in population growth, floodplain development or flood protection through time, since 1) such projections would require assumptions that would be difficult to apply at a national scale across multi-decadal timeframes (e.g., Elmer et al., 2012); and 2) the impacts of those assumptions might obscure the climate change signal we seek to characterize. Our model projections should therefore be considered order-of-magnitude estimates of how differences in emissions scenarios might propagate into changes in flood damages throughout the United States.

2.1 Hydrologic Modeling Inputs

We used spatially and temporally disaggregated precipitation and temperature at 1/8th degree resolution from 29 GCMs and 2 emissions scenarios (RCP4.5 and RCP8.5), generated using the bias correction and spatial disaggregation (BCSD) method (e.g., Wood et al., 2004). The BCSD method uses a quantile mapping approach to match the distribution of GCM-derived monthly outputs to the observed monthly data at a 1-degree resolution in a historical period (1950–2000). It then uses the spatial pattern of daily observations from an analog month as a proxy for sub-grid scale daily (temporal) variability, and scales or shifts these daily observations to ensure that the analog monthly average values match the rescaled GCM output. During the bias correction process (which applies to monthly precipitation and temperature values at the GCM scale), projected precipitation values exceeding the upper end of the climatological range are extrapolated following an extreme value Type I distribution. Additional details of the BCSD weather generation are given in Harding et al. (2012) and Wood and Mizukami (2014).

Catchment hydrology was simulated using the variable infiltration capacity (VIC) hydrologic model (Liang et al., 1994) forced by the BCSD precipitation and temperature fields. The VIC model simulates the range of hydrologic processes relevant to generating runoff, including interception on the forest canopy, evapotranspiration, water storage and melt from snowpack, infiltration, and direct runoff. The runoff component of each model grid cell was remapped to the Hydrologic Response Units (HRUs) defined in the United States Geological Survey (USGS) Geospatial Fabric (GF; Viger and Block, 2014), and then routed through the GF river network using the MizuRoute routing tool, which incorporates both hillslope and river channel

processes (Mizukami et al., 2016a). The GF dataset contains ~57,000 river segments and ~108,000 HRUs (including the right and left bank of most river segments), representing catchments approximately equivalent in area to 12-digit Hydrologic Unit Code basins. The methods used for the downscaling and land surface hydrology were identical to those used in previous studies (e.g., Das et al., 2013; Reclamation, 2014). However, for this effort we used a multi-scale parameter regionalization approach

5   (Samaniego et al., 2010) to improve the spatial coherence of VIC model parameters across basin boundaries (Mizukami et al., In Review). Nash-Sutcliffe Efficiency coefficients indicate that the model adequately captures the magnitude and variability of observed flows across most of the CONUS, while the updated VIC parameters remove some of the artifacts that were observed from the Reclamation (2014) dataset (see Supplemental Information File #1). Full details of the downscaling, VIC model parameters, and routing methodologies are described in Reclamation (2014) and Mizukami et al. (2017), and are

10   summarized in Supplemental Information File #1.

2.2 Modeling Flood Probability

For each of the 58 GCM/RCP combinations in the hydrologic model output, we extracted the time series of annual maximum flow between 1950 and 2099 at each of the ~ 57,000 GF stream locations in the CONUS. Average annual maximum flows in the modeled reaches range from < 5 m^3/s to > 1,000 m^3/s (Figure 1). Prior to generating statistics of peak flows from these

15   events, we plotted the normalized annual maximum time series across all segments and all models (Figure 2). This plot revealed a step in the annual maximum flow time series in the year 2000, which corresponds to the end of the hindcast period used in the BCSD method. This step is even more pronounced in the BCSD precipitation inputs (Figure 3), and most likely reflects the change in how the BCSD method constrains the distribution of events in the historical period compared to in the future period.

20   In order to prevent this artifact from influencing our analysis of future flooding events, we used an early 21st century ensemble average (2001-2020) to represent baseline hydrologic conditions, rather than the more traditional late 20th century baseline. We calculated the magnitude of the "baseline" modeled 1% AEP flood event at each stream segment by fitting a generalized extreme value (GEV) distribution to the full ensemble of annual maximum flow estimates for each RCP over the 2001–2020 period (29 models x 20 years = 580 values), and extracting the 99th percentile value from this model fit. Although the emissions

25   pathways for RCP4.5 and RCP8.5 begin to diverge in 2006, there were no systematic differences between GEV fits for the two RCPs, justifying our treatment of this early 21st century period as a baseline across the full ensemble.

Individual GCMs exhibit a degree of dependence due to shared code, shared scientific literature, shared observations, etc., and as such are not statistically independent (Abramowitz, 2010; Knutti et al., 2010b; Bishop and Abramowitz, 2013). However, the consensus of the community remains that it is best to average across many ensemble members (Tebaldi and Knutti, 2007;

30   Knutti et al., 2010a) as we have done here. From this full ensemble, we evaluated uncertainty in the 1% annual probability event by bootstrapping (see Supplemental Information File #2). Based on these analyses, we expect the sample uncertainty on our 1% AEP flood event to be in the range of 5–20%. As shown later, the variability in the multimodel GCM ensemble is

much larger than this uncertainty in the GEV fits, so we did not propagate this source of uncertainty through all of our calculations.

To estimate future flood frequency and damages through the 21st century, we compared the full transient of future annual streamflow maxima for each GCM/RCP combination to the baseline 1% AEP event. In all of the summaries that follow, we

5   define a "flood" at a given stream segment as an annual maximum flow value that exceeds the baseline 1% AEP event at that segment. The comparison between future flows and the 1% AEP threshold yields a time series of floods at each segment, as well as an estimate of the total number of flood events nationwide in each year. At each segment, we also calculated an ensemble average probability of exceeding the 1% AEP event in each year, by tabulating the fraction of models experiencing a flood and smoothing these probabilities over a 20-year moving window. These time- and ensemble-averaged flood

10   probabilities by segment were then linked to the assets exposed within each floodplain to calculate projected annual damages, as summarized below.

2.3 Asset Exposure and Damages

We estimated asset damages resulting from current 1% AEP flood events using data from an experimental tool under development for the U.S. Army Corps of Engineers Institute for Water Resources (IWR, 2014). For this tool, we compiled all

15   of the 1% AEP floodplains as mapped by FEMA and included in the National Flood Hazard Layer (NFHL). We then used a series of steps to calculate the depth of flooding and resulting damages from 1% AEP events, and merged this information with the flood probabilities described in Section 2.2. A brief summary of the flood damage calculations follows. Supplemental Information File #2 provides more complete details of the flood damage calculations.

2.3.1 Cataloguing Damages by Flood Zone

20   To catalog damages by flood zone, we intersected 1% AEP flood boundaries with Census blocks to create a set of flood zone polygons subdivided by Census block boundaries. Within each of these flood zone/Census block units, we calculated the distribution of flood depths for the 1% AEP event using the National Elevation Dataset (NED; USGS, 2016). We then merged this information with land cover data from the National Land Cover Dataset (Homer et al., 2015) to determine the distribution of flood depths within "developed" portions of each Census block, and estimated exposure of built assets using FEMA's

25   HAZUS-MH General Building Stock inventory (FEMA, 2009). The General Building Stock inventory provides estimates of the number and aggregate dollar value of multiple types of residential, commercial, and industrial buildings for each Census block.

For the developed portion of each Census block/floodzone intersection, we created damage estimates using depth-damage functions from USACE and FEMA (FEMA, 2009; USACE, 2000, 2003). A separate depth-damage function was used for each

30   of 28 different categories of buildings (e.g., residential one-story homes without a basement). Each depth-damage function describes the percent loss as a function of depth. The depth-damage functions were applied to the aggregate value for each building category within each NFHL-Census block intersection, using the depth exposure results described above.

2.3.2 Aggregating Damages to National Scale

Once the damage estimates were generated for each Census block/floodplain intersection, we aggregated this information up to the same HRUs that were used in the hydrologic analysis. We then linked each stream segment at which flood statistics were calculated back to the total asset damages resulting from a 1% AEP event at that location. Figure 4 shows the total damages expected from 1% AEP events at each of the HRUs across the CONUS.

For each GCM, we combined the timeseries of floods at each stream segment with the assets exposed in that HRU to compute a timeseries of monetary damages. When averaged across all nodes in the CONUS, this approach yielded a relatively smooth curve of CONUS-wide monetary damages through the 21st century. However, this approach treats the hydrologic timeseries from each GCM as a deterministic, rather than a probabilistic, projection of future conditions. In order to use the full ensemble of GCMs in a more probabilistic framework, we used a Monte Carlo approach. We simulated 1,000 100-year time series of flood damages in the CONUS using the ensemble average probability of exceeding the 1% AEP event at each segment in each year. This yielded a distribution of flood damages in each year, from which we extracted a minimum, maximum, and ensemble average for each of the RCPs.

2.4 Uncertainties

Each of the methodological steps outlined above introduces uncertainties into our analysis. While it may not be possible to quantify all of these uncertainties, we summarize each of them here along with our best judgement on the magnitude and directionality of their impacts.

First, GCMs have historically not resolved precipitation well (e.g., Flato et al., 2013), such that downscaling is required to simulate catchment hydrology at a physically meaningful scale. Although the BCSD method has been used in the past to account for precipitation changes in hydrologic modeling applications (e.g., Das et al., 2013; Shrestha et al., 2014; Ning et al., 2015), downscaling methods are themselves imperfect. While BCSD has been shown to have fewer artifacts in historical climate compared to other commonly used methods (e.g., Gutmann et al., 2014), our analysis shows that the BCSD method does introduce an artifact into the precipitation time series between historical and future projections, which is not well understood (see Figures 2-3). Our use of an early 21st century "baseline" to circumvent this artifact is likely to be conservative, since it reduces the magnitude of climate changes since the mid-20th century. Furthermore, since precipitation extremes are likely to increase more quickly than averages in the future (e.g., Kendon et al., 2014; Prein et al., 2016), our reliance on BCSD downscaling to drive future hydrologic changes is likely to underestimate changes in hydrologic extremes through time.

Second, the choice of hydrologic model will introduce uncertainty into our analysis (e.g., Mendoza et al., 2015; 2016; Mizukami et al., 2016b). Comparison of hydrologic results from different VIC parameter sets indicates that the choice of hydrologic model parameters within the VIC modeling framework does not substantially change the model's ability to simulate natural flows (see Supplemental Information File #1), though it may alter model performance at specific locations or times. However, because our method includes spatially explicit estimates in flooding and damages, the direction and magnitude of

impact from selection of a different hydrologic model would depend on how differently an alternative hydrologic model simulates relevant hydrologic processes in different regions, and is therefore difficult to estimate *a priori*.

Third, because the 1% AEP (100 year return interval) floodplains are the only flood risk zones consistently mapped at a national scale, our model tabulates damages only within these mapped floodplains. Consideration of a wider range of flood magnitudes would increase modeled damages under both baseline and future scenarios, since floods smaller and larger than 1% AEP events will also generate monetary damages. The relative change in future vs baseline flood damages across a full range of flood magnitudes would depend on the spatial distribution of built assets in each modeled reach, and how the relative change in smaller (e.g., 25-year) vs larger (e.g., 500-year) events interact with this distribution of built assets. In addition, because the calculations of the baseline 1% AEP event and future exceedances are each based on an annual maximum timeseries, we did not consider the possibility of multiple flood events in any one year. Although the occurrence of multiple 1% AEP events in one year is unlikely, this choice will make our future damage estimates conservative, since the frequency of flooding generally increases through the 21st century, as summarized below.

Finally, we did not propagate projected changes in population, floodplain development, or flood protection through our analysis. We also restricted our analysis to a single set of damage functions (FEMA, 2009) and did not incorporate sensitivities to different types of damage functions into our analysis (e.g., Bubeck et al., 2011). We made these simplifying assumptions so that we could isolate the effects of hydrologic changes, which are themselves uncertain, from the effects of socioeconomic changes or engineering investments, which may be impossible to predict. For example, while increased development in flood-prone areas could increase exposure of built assets to increased flooding (e.g., Liu et al., 2015), flood protection investments that decrease exposure may be equally likely. Because the uncertainties in socioeconomic projections and future changes to floodplain management could potentially overwhelm the uncertainties in our hydrologic model outputs, our results rely on the simplifying assumption that the built environment remains static through the 21st century. Over the past century, development appears to have contributed to increased flood damage costs (e.g., Pielke and Downton, 2000), so to the extent that human behavior remains unchanged, it is likely that our assumption underestimates future costs.

Despite these uncertainties, CONUS-wide annual inland flooding damages estimated using our approach are very similar to inland flooding damages observed over the 20th and early 21st century, as summarized below. Based on this observation and the caveats summarized above, we expect that our nationwide projections represent at least order-of-magnitude estimates of historical and future flood damages.

3 Results

3.1 Flood Frequency Projections

Since the hydrographs generated by the downscaled hydrology outputs are unique to each GCM/RCP combination, each model also produces its own time series of flooding at each stream segment. As one way of summarizing these data, we calculated the total number of flood events across the CONUS in each year of each model simulation. We then summarized the

distribution of the total number of flood events across all 29 GCMs for each RCP (Figure 5). As expected based on our method, the annual number of 1% AEP floods across the CONUS across all models averages approximately 500 events between 2000 and 2020 (~1% of the ~ 57,000 segments in the CONUS). This average number of floods increases to approximately 750 events by 2100 under RCP4.5, and up to approximately 1,250 events under RCP8.5.

5   Because a "flood" as defined here is threshold-dependent, uncertainty in the magnitude of the 1% AEP event will affect the exact timeseries of floods at each node for each model. We explored the effects of this threshold dependence on the number of floods occurring in each year by introducing a random error of +/-20% into the magnitude of the 1% AEP event at each node (based on our bootstrapping analysis), and re-calculating the timeseries of flooding at each node. At a national scale, the effect of this error analysis on the timeseries of flooding is overwhelmed by the inter-model variability in peak flows (see

10   Supplemental Information File #2). As a result, we did not conduct further uncertainty analysis related to the calculation of the 1% AEP flood event.

Using the time series of flooding for each segment and combining these values across all models, we calculated an average flood frequency by segment for 20-year intervals in the baseline (2001–2020), mid-century (2040–2059), and late century (2080–2099). This allowed us to calculate an ensemble-averaged change in flood frequency for each segment, to evaluate

15   where there may be spatially coherent patterns of increased flood risk. As shown in Figure 6, the largest fractional changes in flood frequency across the CONUS occur in the southern Appalachians and Ohio River valley, the northern and central Rocky Mountains, and the Northwest. In each of these regions, the ensemble average across models suggests that historical 1% AEP events could become 2–5 times more frequent by the end of the century.

In some regions of the United States (e.g., the southern Appalachians and northern Rocky Mountains), the spatial patterns of

20   increased flood frequency can be explained by the increased occurrence of extreme precipitation events projected by the GCM-derived precipitation outputs. In other regions such as the Sierras and the Cascades, increases in the frequency of flood events are not as easily explained by changes in precipitation alone. In these locations, the increase in frequency of extreme floods more likely reflects changes in the nature of winter precipitation (rain vs snow) compared to baseline conditions (e.g., Das et al., 2013).

25   **3.2 Flood Damage Projections**

By combining the changes in frequency of flooding at each segment with the asset exposure and damage associated with each floodplain, we generated a full time series of projected changes in flood damages across the CONUS through the 21st century. Figure 7 shows the results from 1,000 individual simulations of nationwide flood damages using the probability of flooding at each segment, as described in Section 2.3.2. Since we assume no changes in built assets or flood protection within mapped

30   floodplains, changes in flood damages broadly mimic changes in flood frequency at a national scale (Figure 7; compare to Figure 5), with minor differences between these trends reflecting the way that regional trends in flood frequency interact with asset exposure within 1% AEP floodplains (see Figure 4). Expected annual flood damages under the RCP4.5 scenario increase from approximately $3 billion between 2000 and 2020 to approximately $4 billion by the end of the century. Under the

RCP8.5 scenario, expected annual flood damages increase from approximately $3 billion in the early 21st century to over $7 billion by 2100. The modeled damage distribution in the early part of the 21st century also closely approximates the distribution of observed annual damages over the late 20th century (e.g., NOAA, 2016).

Figure 7 also highlights how different GHG emissions pathways generate different trajectories of flood damages through the remainder of the 21st century. While the RCP4.5 and RCP8.5 pathways are generally similar through mid-century, the damage trajectories under the two emissions scenarios begin to diverge in the latter half of the 21st century. By 2075, the average annual difference between flood damages under the RCP4.5 and RCP8.5 emissions pathways is approximately $2 billion, and by 2100 this difference grows to almost $4 billion.

The increasing flood damages under RCP8.5 relative to RCP4.5 are not evenly distributed throughout the United States. Figure 8 shows the time series of average annual damages in each region of the CONUS. As shown in Figure 8, the most significant differences between projected flood damages under the two emissions scenarios are in the Southeast, where the difference between the two trajectories approaches $1.5 billion per year by the end of the century; and in the Northeast and Midwest, where the difference between the two scenarios is close to $750 million per year by 2100. Although there are also differences in damages between the two emissions scenarios in other regions, these differences are generally small relative to those three regions of the country. The increasing flood damages projected for the Southeast, Northeast and Midwest are consistent with increases in modeled changes in annual maximum precipitation throughout the eastern United States, as described in the third National Climate Assessment (e.g., Walsh et al., 2014), combined with the high value of built assets within floodplains in these regions relative to the rest of the nation (see Figure 4).

4 Discussion and Conclusions

Based on our model, we find that if future GHG emissions remain unchecked, monetary damages from flooding throughout the CONUS are likely to increase through the 21st century. Global GHG reductions, represented by RCP4.5, could limit these increasing flood damages, potentially saving billions of dollars per year (in undiscounted 2014 dollars) by the end of the century. To our knowledge, this study is the first to link spatially explicit hydrologic projections from a full ensemble of climate model projections to mapped assets in order to estimate future flood damages at a national scale.

Although this study represents a significant methodological advance in projecting future inland flooding damages nationwide, there are a number of avenues for future work. As summarized in Section 2.4, these avenues include further exploration of different downscaling methods; consideration of different hydrological models; and simulation of a wider range of flood magnitudes and the intersection of these flood zones with built assets.

Preliminary analysis of precipitation outputs from the newer localized constructed analogue downscaling method (LOCA: Pierce et al., 2014) suggests that artifacts introduced by the BCSD method are likely to exist in other products as well. Ideally, future hydrologic projections could be driven by a dynamically downscaled climate model to avoid the artifacts introduced from statistical downscaling. However, full dynamical downscaling through the 21st century at the scale of the CONUS may

remain computationally prohibitive for a number of years to come (see for example Liu et al., 2016). In the interim, future work could replicate the method described here using quasi-dynamical downscaling methods (e.g., Gutmann et al., 2016).

With the exception of limited mapping of 500-year floodplains, there is no national data available to evaluate how damages might increase with increasing flood magnitude above or below the 1% AEP event. However, there are some locations in the
5   United States where floodplains are mapped at a range of magnitudes both above and below the 1% AEP event (FEMA, 2014). Case studies from these locations could allow us to explicitly model the damages encompassed by these smaller and larger events, and evaluate local changes in flood damages driven by a wider range of flood events.

Finally, we stress that even if global GHG emissions are substantially reduced, there is no *a priori* way to predict how humans will adapt to future flood risk under any emissions scenario. As summarized in Section 2.4, future demographic and
10   infrastructure changes could either increase or decrease damages from flooding in the future: increased flood protection measures could decrease damages, while increases in development in flood-prone areas could increase them. While our modeling indicates that nationwide exposure to flooding will increase through the 21st century, the overall damages incurred will depend both on how we alter our emissions, and how we adapt to changing risks of future flooding.

Acknowledgements

15   The authors acknowledge financial support from the U.S. Environmental Protection Agency's Office of Atmospheric Programs (contract # EP-BPA-12-H-0024) and the U.S. Army Corps of Engineers (contract # W912HQ-10-D-0005). The views expressed in this article are solely those of the authors, and do not necessary represent those of their employers. The National Center for Atmospheric Research is sponsored by the National Science Foundation.

References

20   Abramowitz, G.: Model independence in multi-model ensemble prediction, Australian Meteorological and Oceanographic Journal, 59, 3–6, 2010.

Archfield, S. A., Hirsch, R. M., Viglione, A., and Blöschl, G.: Fragmented patterns of flood change across the United States, Geophysical Research Letters, 43, 19, 2016.

Arnell, N. W. and Gosling, S. N.: The impacts of climate change on river flood risk at the global scale, Climatic Change, 134,
25   3:387–401, 2016.

Berghuijs, W.R., Woods, R.A., Hutton, C.J. and Sivapalan, M.:Dominant flood generating mechanisms across the United States. Geophysical Research Letters, 43(9), pp.4382-4390. 2016.

Bishop, C. H. and Abramowitz, G.: Climate model dependence and the replicate Earth paradigm, Clim Dyn, 41(3-4), 885–900, doi:10.1007/s00382-012-1610-y, 2013.

Bubeck, P., de Moel, H., Bouwer, L.M.., and Aerts, J.C.: How reliable are projections of future flood damage? Natural Hazards and Earth System Sciences, 11, 3293-3306, 2011.

Das, T., Maurer, E. P., Pierce, D. W., Dettinger, M. D., and Cayan, D. R.: Increases in flood magnitudes in California under warming climates, Journal of Hydrology, 501, 101–110, 2013.

5 Downton, M. W., Miller, J. Z. B., and Pielke Jr., R. A.: Reanalysis of US National Weather Service flood loss database, Natural Hazards Review, 6, 1:13–22, 2005.

Elmer, F., Hoymann, J., Duthmann, D., Vorogushyn, S., and Kreibich, H.: Drivers of flood risk change in residential areas. Natural Hazards and Earth System Sciences, 12, 1641-1657, 2012.

FEMA: Multi-Hazard Loss Estimation Methodology, Flood Model, HAZUS-MH MR4, Technical Manual, Federal
10 Emergency Management Agency, Washington, DC, 2009.

FEMA: Risk MAP Flood Risk Products Factsheet. Federal Emergency Management Agency, Washington, DC. Available: https://www.fema.gov/media-library/assets/documents/22454, 2014.

Flato, G., Marotzke, J., Abiodun, B., Braconnot, P., Chou, S.C., Collins, W., Cox, P., Driouech, F., Emori, S., Eyring, V., Forest, C., Gleckler, P., Guilyardi, E., Jakob, C., Kattsov, V., Reason, C., and Rummukainen, M.: Evaluation of climate models,
15 In *Climate Change 2013: The Physical Science Basis. Contribution of Working Group I to the Fifth Assessment Report of the Intergovernmental Panel on Climate Change,* T. F. Stocker, Qin, D., Plattner, G. -K., Tignor, M., Allen, S. K., Boschung, J., Nauels, A., Xia, Y., Bex, V., and Midgley, P. M. (eds.), Cambridge University Press, Cambridge, United Kingdom and New York, NY, USA, 2013.

Fortune: North Carolina Estimates $1.5 Billion in Damage from Hurricane Matthew, Available:
20 http://fortune.com/2016/10/17/hurricane-matthew-north-carolina-damage/, 2016.

Gosling, S. N., Bretherton, D., Haines, K., and Arnell, N. W.: Global hydrology modelling and uncertainty: Running multiple ensembles with a campus grid, Philos. Trans. R. Soc. A Math. Phys. Eng. Sci., 368, 4005–4021, 2010.

Gutmann, E., Barstad, I., Clark, M., Arnold, J., and Rasmussen, R.: The Intermediate Complexity Atmospheric Research Model (ICAR), Journal of Hydrometeorology, 17, 3:957–973, doi: 10.1175/JHM-D-15-0155.1, 2016.
25 Gutmann, E., Pruitt, T., Clark, M. P., Brekke, L., Arnold, J. R., Raff, D. A., and Rasmussen, R. M.: An intercomparison of statistical downscaling methods used for water resource assessments in the United States, Water Resources Research, 50, 9:7167–7186, doi: 10.1002/2014WR015559, 2014.

Harding, B. L., Wood, A W, and Prairie, J R.: The implications of climate change scenario selection for future streamflow projection in the Upper Colorado River Basin, Hydrol. Earth Syst. Sci., 16, 3989-4007, doi:10.5194/hess-16-3989-2012, 2012.
30 Hirabayashi, Y., Kanae, S., Emori, S., Oki, T., and Kimoto, M.: Global projections of changing risks of floods and droughts in a changing climate, Hydrological Sciences Journal, 53, 4:754–772, 2008.

Hirabayashi, Y., Mahendran, R., Koirala, S., Konoshima, L., Yamazaki, D., Watanabe, S., Kim, H., and Kanae, S.: Global flood risk under climate change, Nature Climate Change, 3, 9:816–821, 2013.

Hirsch, R.M. and Ryberg, K.R.: Has the magnitude of floods across the USA changed with global CO_2 levels? Hydrological Sciences Journal, 57, 1:1–9, 2012.

Homer, C. G., Dewitz, J. A., Yang, L., Jin, S., Danielson, P., Xian, G., Coulston, J., Herold, N. D., Wickham, J. D., and Megown, K.: Completion of the 2011 National Land Cover database for the conterminous United States – representing a decade of land cover change information, Photogrammetric Engineering and Remote Sensing, 81, 5:345–354, 2015.

IPCC: *Managing the Risks of Extreme Events and Disasters to Advance Climate Change Adaptation. A Special Report of Working Groups I and II of the Intergovernmental Panel on Climate Change*, Field, C. B., Barros, V., Stocker, T. F., Qin, D., Dokken, D. J., Ebi, K. L., Mastrandrea, M. D., Mach, K. J., Plattner, G. -K., Allen, S. K., Tignor, M., and Midgley, P. M. (eds.): Cambridge University Press, Cambridge, UK, and New York, NY, USA, 2012.

IWR (2014). "National Flood Risk Characterization Tool: Overview of Capabilities and Current Limitations." Presentation at an Inter-agency flood risk characterization workshop, February 25, 2014. Available at: http://www.iwr.usace.army.mil/Portals/70/docs/frmp/Flood_Risk_Char/NFRCT_Slides_FRM_wkshp_v1.pdf.

Kendon, E. J., Roberts, N. M., Fowler, H. J., Roberts, M. J., Chan, S. C., and Senior, C. A.: Heavier summer downpours with climate change revealed by weather forecast resolution model, Nature Climate Change, 4, 7:570–576, doi: 10.1038/NCLIMATE2258, 2014.

Knutti, R., G. Abramowitz, M. Collins, V. Eyring, P.J. Gleckler, B. Hewitson, and L. Mearns.: Good Practice Guidance Paper on Assessing and Combining Multi Model Climate Projections. In: Meeting Report of the Intergovernmental Panel on Climate Change Expert Meeting on Assessing and Combining Multi Model Climate Projections [Stocker, T.F., D. Qin, G.-K. Plattner, M. Tignor, and P.M. Midgley (eds.)]. IPCC Working Group I Technical Support Unit, University of Bern, Bern, Switzerland, 2010.

Kundzewicz, Z. W., Kanae, S., Seneviratne, S. I., Handmer, J., Nicholls, N., Peduzzi, P., Mechler, R., Bouwer, L. M., Arnell, N., Mach, K., and Muir-Wood, R.: Flood risk and climate change: Global and regional perspectives, Hydrological Sciences Journal, 59, 1:1–28, 2014.

LED: The Economic Impact of the August 2016 Floods on the State of Louisiana, Prepared by Lewis Terrell and Associate, LLC for the Louisiana Economic Development, Available: http://gov.louisiana.gov/assets/docs/RestoreLA/SupportingDocs/Meeting-9-28-16/2016-August-Flood-Economic-Impact-Report_09-01-16.pdf, 2016.

Liang, X., Lettenmaier, D. P., Wood, E. F., and Burges, S. J.: A simple hydrologically based model of land surface water and energy fluxes for general circulation models, Journal of Geophysical Research, 99, D7:14415–14428, doi: 10.1029/94JD00483, 1994.

Lins, H. F. and Slack, J. R.: Streamflow trends in the United States, Geophysical Research Letters, 26, 2:227–230, 1999.

Mallakpour, I. and Villarini, G.: The changing nature of flooding across the central United States, Nature Climate Change, 5, 3:250–254, 2015.

Maurer, E.P., Wood, A.W., Adam, J.C., Lettenmaier, D.P., and Nijssen, B.: A long-term hydrologically-based dataset of land surface fluxes and states for the Conterminous United States, Journal of Climate 15: 3237-3251, 2002.

Liu, C., Ikeda, K., Rasmussen, R., Barlage, M., Newman, A. J., Prein, A. F., Chen, F., Chen, L., Clark, M., Dai, A., Dudhia, J., Eidhammer, T., Gochis, D., Gutmann, E., Kurkute, S., Li, Y., Thompson, G. and Yates, D.: Continental-scale convection-permitting modeling of the current and future climate of North America, Clim Dyn, 1–25, doi:10.1007/s00382-016-3327-9, 2016.

Liu, J., Hertel, T., Diffenbaugh, N., Delgado, M., and Ashfaq, M: Future property damage from flooding: sensitivities to economy and climate change. Climatic change 132: 741-749, 2015.

McCabe, G. J. and Wolock, D. M.: A step increase in streamflow in the conterminous United States, Geophysical Research Letters, 29, 24, 2002.

Mendoza, P. A., Clark, M. P., Mizukami, N., Gutmann, E. D., Arnold, J. R., Brekke, L. D. and Rajagopalan, B.: How do hydrologic modeling decisions affect the portrayal of climate change impacts? Hydrological Processes, 30(7), 1071–1095, doi:10.1002/hyp.10684, 2016.

Mendoza, P. A., Clark, M. P., Mizukami, N., Newman, A. J., Barlage, M., Gutmann, E. D., Rasmussen, R. M., Rajagopalan, B., Brekke, L. D. and Arnold, J. R.: Effects of Hydrologic Model Choice and Calibration on the Portrayal of Climate Change Impacts, J. Hydrometeor, 16(2), 762–780, doi:10.1175/JHM-D-14-0104.1, 2015.

Mizukami, N., Clark, M. P., Newman, A. J., Wood, A., Gutmann, E. D., Nijssen, B., Rakovec, O., and Samaniego, L.: Towards Seamless Large Domain Parameter Estimation for Hydrologic Models, Water Resources Research 53. Doi: 10.1002/2017WR020401, 2017.

Mizukami, N., Clark, M., Gutmann, E., Mendoza, P., Newman, A. J., Nijssen, B., Livneh, B., Hay, L. E., Arnold, J. R., and Brekke, L. D.: Implications of the methodological choices for hydrologic portrayals of climate change over the contiguous United States: Statistically downscaled forcing data and hydrologic models, Journal of Hydrometeorology, 7, 73–98, 2016a.

Mizukami, N., Clark, M. P., Viger, R. J., Markstrom, S. L., Hay, L. E., Arnold, J. R., and Brekke, L. D.: MizuRoute version 1: A river network routing tool for a continental domain water resources applications, Geoscientific Model Development, 9, 6:2223, 2016b.

National Academies of Sciences, Engineering, and Medicine: *Attribution of extreme weather events in the context of climate change,* National Academies Press, 2016.

Ning, L., Riddle, E. E., and Bradley, R. S.: Projected changes in climate extremes over the northeastern United States, Journal of Climate, 28, 8:3289–3310, 2015.

NOAA: Hydrologic Information Center Flood Loss Data, National Oceanic and Atmospheric Administration, Silver Spring, MD, Available: http://www.nws.noaa.gov/hic/, 2016.

Pielke Jr., R. A. and Downton, M. W.: Precipitation and damaging floods: Trends in the United States, 1932–97, Journal of Climate, 13, 20:3625–3637, 2000.

Pierce, D. W., Cayan, D. R., and Thrasher, B. L.: Statistical downscaling using localized constructed analogs (LOCA), Journal of Hydrometeorology, 15, 6:2558–2585, doi: 10.1175/JHM-D-14-0082.1, 2014.

Prein, A. F., Rasmussen, R. M., Ikeda, K., Liu, C., Clark, M. P., and Holland, G. J.: The future intensification of hourly precipitation extremes, Nature Climate Change, doi: 10.1038/NCLIMATE3168, 2016.

5   Reclamation: Downscaled CMIP3 and CMIP5 Climate and Hydrology Projections: Release of Hydrology Projections, Comparison with Preceding Information, and Summary of User Needs, Prepared by the U.S. Department of the Interior, Bureau of Reclamation, Technical Services Center, Denver, CO, 2014.

Samaniego, L., Kumar, R., and Attinger, S.: Multiscale parameter regionalization of a grid-based hydrologic model at the mesoscale, Water Resources Research, 46, 5, doi: 10.1029/2008WR007327, 2010.

10   Shrestha, R. R., Schnorbus, M. A., Werner, A. T., and Zwiers, F. W.: Evaluating hydroclimatic change signals from statistically and dynamically downscaled GCMs and hydrologic models, Journal of Hydrometeorology, 15, 2:844–860, 2014.

Tebaldi, C. and Knutti, R.: The use of the multi-model ensemble in probabilistic climate projections, Philosophical Transactions of the Royal Society a-Mathematical Physical and Engineering Sciences, 365(1857), 2053–2075, doi:10.1098/rsta.2007.2076, 2007.

Trenberth, K. E., Fasullo, J. T., and Shepherd, T. G.: Attribution of climate extreme events, Nature Climate Change, 5,725–730, doi: 10.1038/nclimate2657, 2015.

15   USACE: Economic Guidance Memorandum (EGM 01-03): Generic Depth-Damage Relationships, U.S. Army Corps of Engineers, Available: https://planning.erdc.dren.mil/toolbox/library/EGMs/egm01-03.pdf, 2000.

USACE: Economic Guidance Memorandum (EGM) 04-01, Generic Depth-Damage Relationships for Residential Structures with Basements, U.S. Army Corps of Engineers, Available: https://planning.erdc.dren.mil/toolbox/library/EGMs/egm04-01.pdf, 2003.

20   U.S. Global Change Research Program (USGCRP), 2015: U.S. Global Change Research Program General Decisions Regarding Climate-Related Scenarios for Framing the Fourth National Climate Assessment. USGCRP Scenarios and Interpretive Science Coordinating Group. Available online at https://scenarios.globalchange.gov/accouncement/1158

USGS: National Elevation Dataset (NED), U.S. Department of the Interior, U.S. Geological Survey, Available: https://lta.cr.usgs.gov/NED, 2016.

25   Viger, R. J. and Bock, A.: GIS Features of the Geospatial Fabric for National Hydrologic Modeling, U.S. Geological Survey, Available: http://dx.doi.org/doi:10.5066/F7542KMD, 2014.

Walsh, J., D. Wuebbles, K. Hayhoe, J. Kossin, K. Kunkel, G. Stephens, P. Thorne, R. Vose, M. Wehner, J. Willis, D. Anderson, S. Doney, R. Feely, P. Hennon, V. Kharin, T. Knutson, F. Landerer, T. Lenton, J. Kennedy, and R. Somerville: Climate Change

30   Impacts in the United States: The Third National Climate Assessment. Ch. 2: Our Changing Climate. J. M. Melillo, Terese (T.C.) Richmond, and G. W. Yohe, Eds., U.S. Global Change Research Program, 19-67. doi:10.7930/J0KW5CXT., 2014.

Wobus, C., Lawson, M., Jones, R., Smith, J., and Martinich, J.: Estimating monetary damages from flooding in the United States under a changing climate, Journal of Flood Risk Management, 7, 3:217–229, 2014.

Wood, A. W., Leung, L. R., Sridhar, V., and Lettenmaier, D. P.: Hydrologic implications of dynamical and statistical approaches to downscaling climate model outputs, Climatic Change, 62, 1–3:189–216, 2004.

Wood, A.W. and Mizukami, N.: CMIP5 1/8th Degree Daily Weather and VIC Hydrology Datasets for CONUS, NCAR Final Project Report to USACE Responses to Climate Change Project (W26HM423495778), 32 pages, 2014.
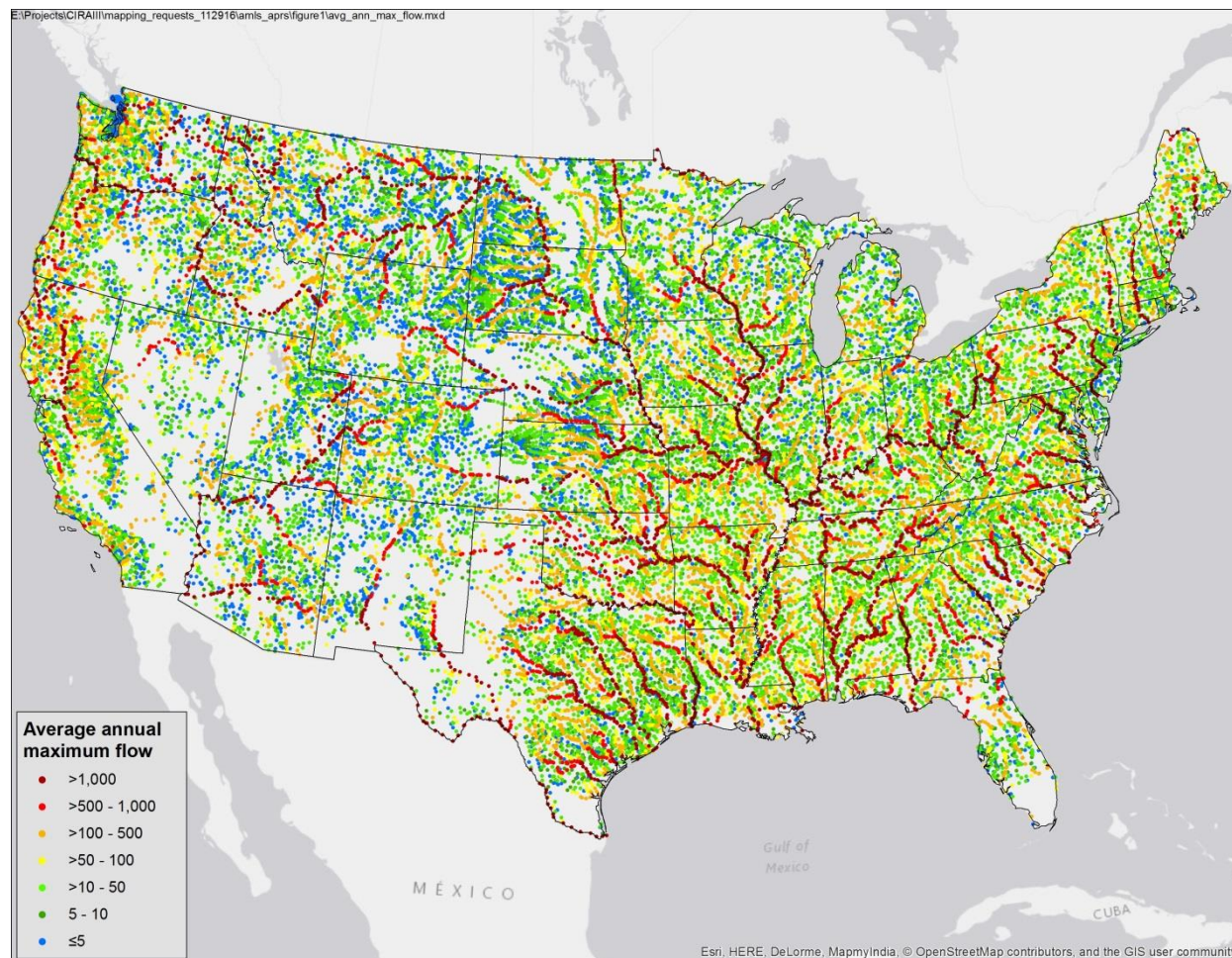
Figure 1: Locations of the 57,116 stream segment with hydrologic projections used in our analysis. Color corresponds to the baseline average annual maximum flow for each segment, in m^3s^{-1}.
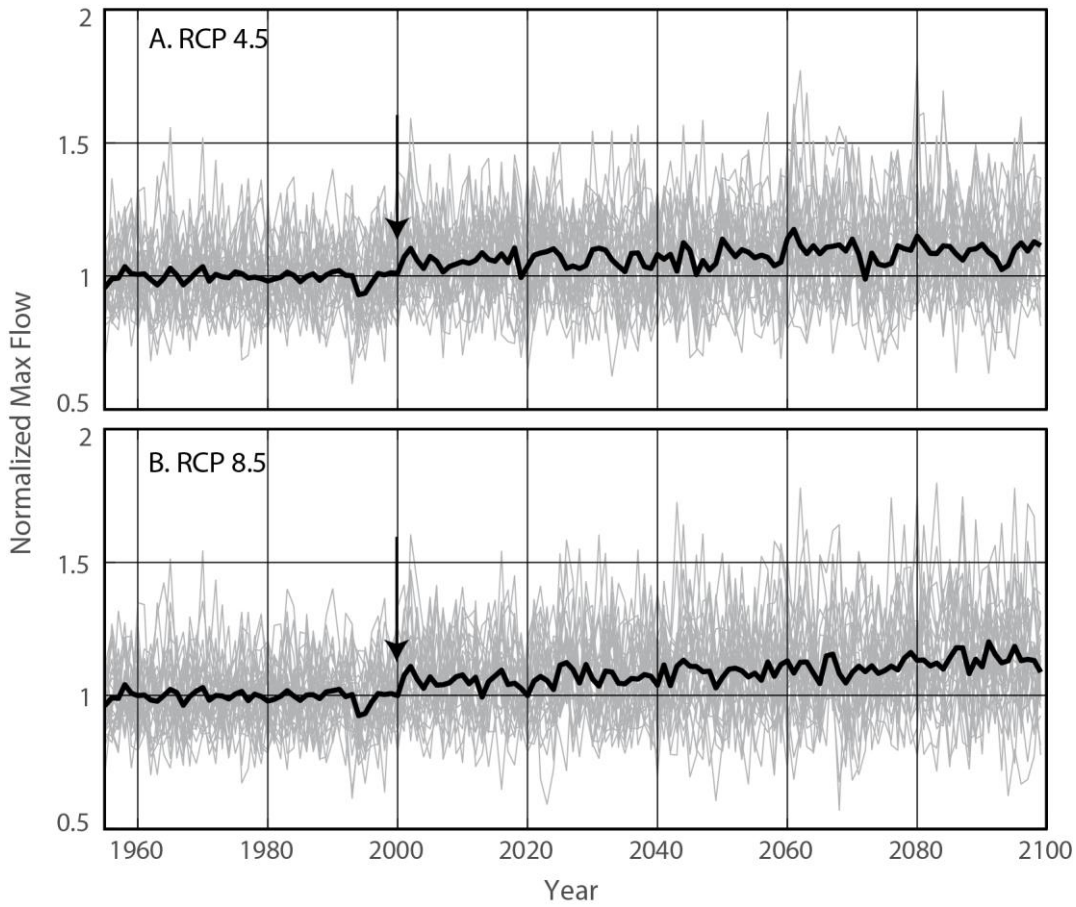
Figure 2: Trends in annual maximum flow across all stream segments in the CONUS. Thin grey lines represent annual maximum flow normalized to 2001–2020 mean, and averaged across all segments for each individual model. Thick black line represents ensemble average. Step increase in the year 2000 for both RCPs (black arrow) is an artifact of the BCSD method. Accordingly, the "baseline" 1% AEP event was calculated from an early 21st century ensemble (see text).
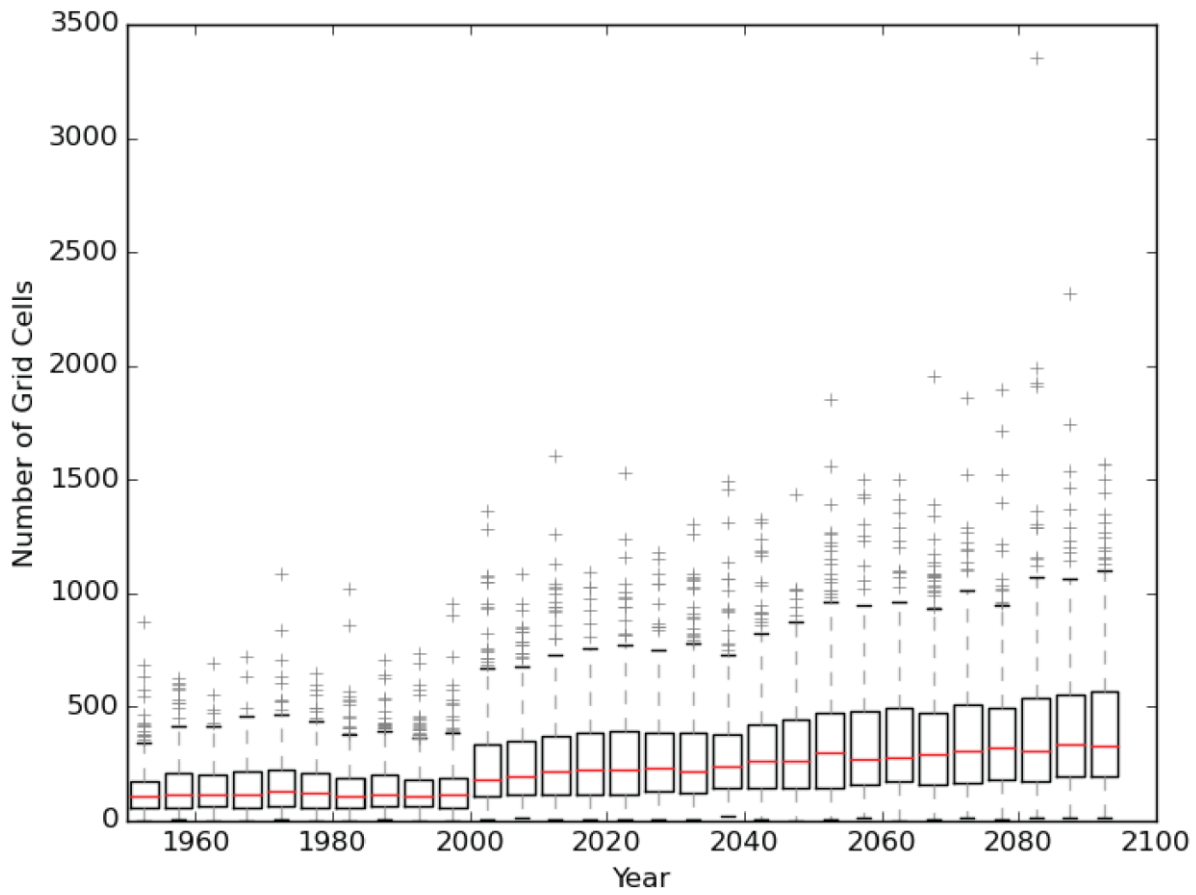
Figure 3: Number of BCSD grid cells in CONUS experiencing their maximum daily precipitation in each year between 1950 and 2100 per model. Box and whiskers represent spread across all of the individual models used in the flow simulations. The step in the year 2000 is an artifact of the BCSD method (p value <0.001). "Baseline" 1% AEP event was calculated using the years 2001-2020.
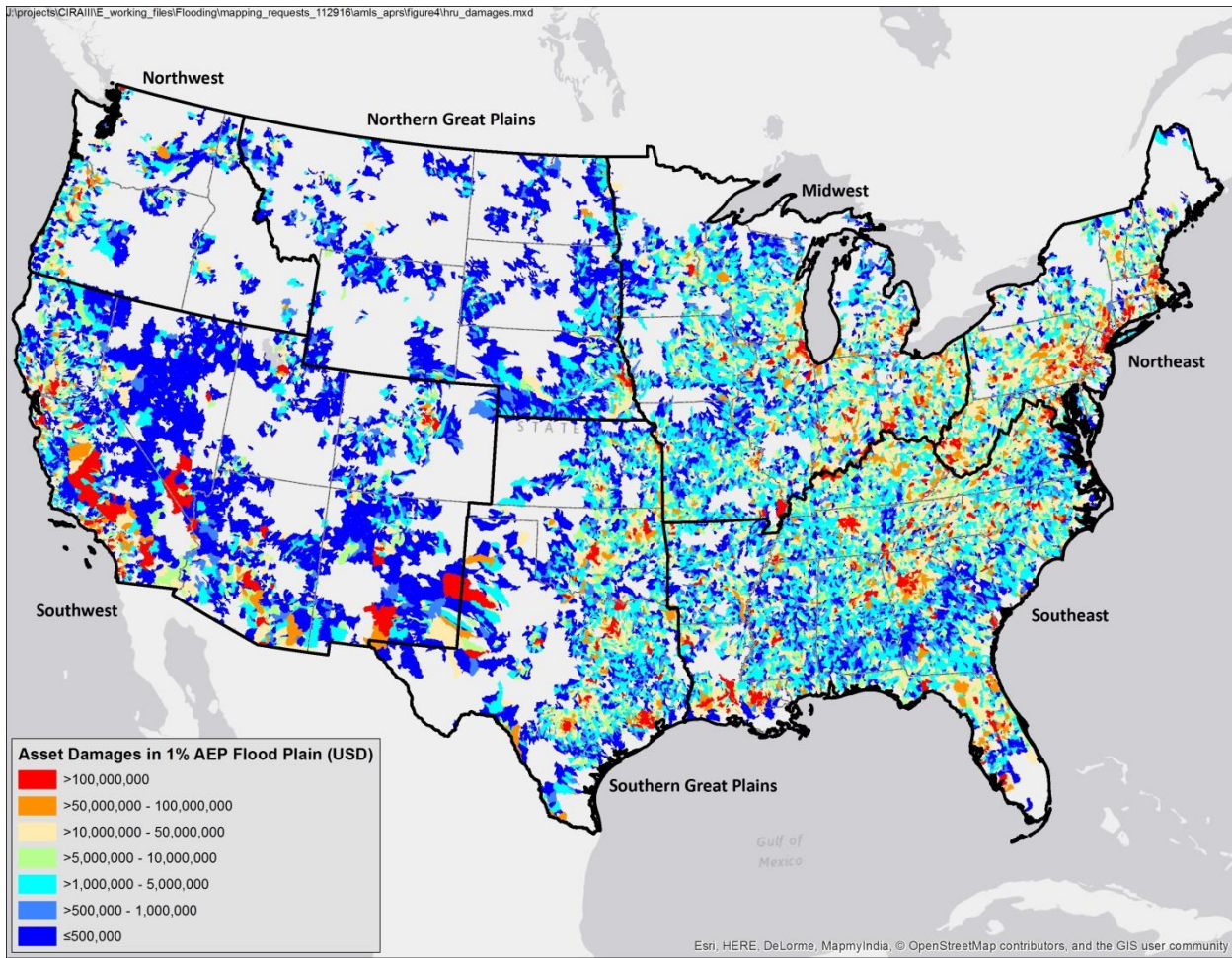
Figure 4: Total asset damages from a 1% AEP flood event in each of the HRUs in the CONUS. Values in 2014 dollars.
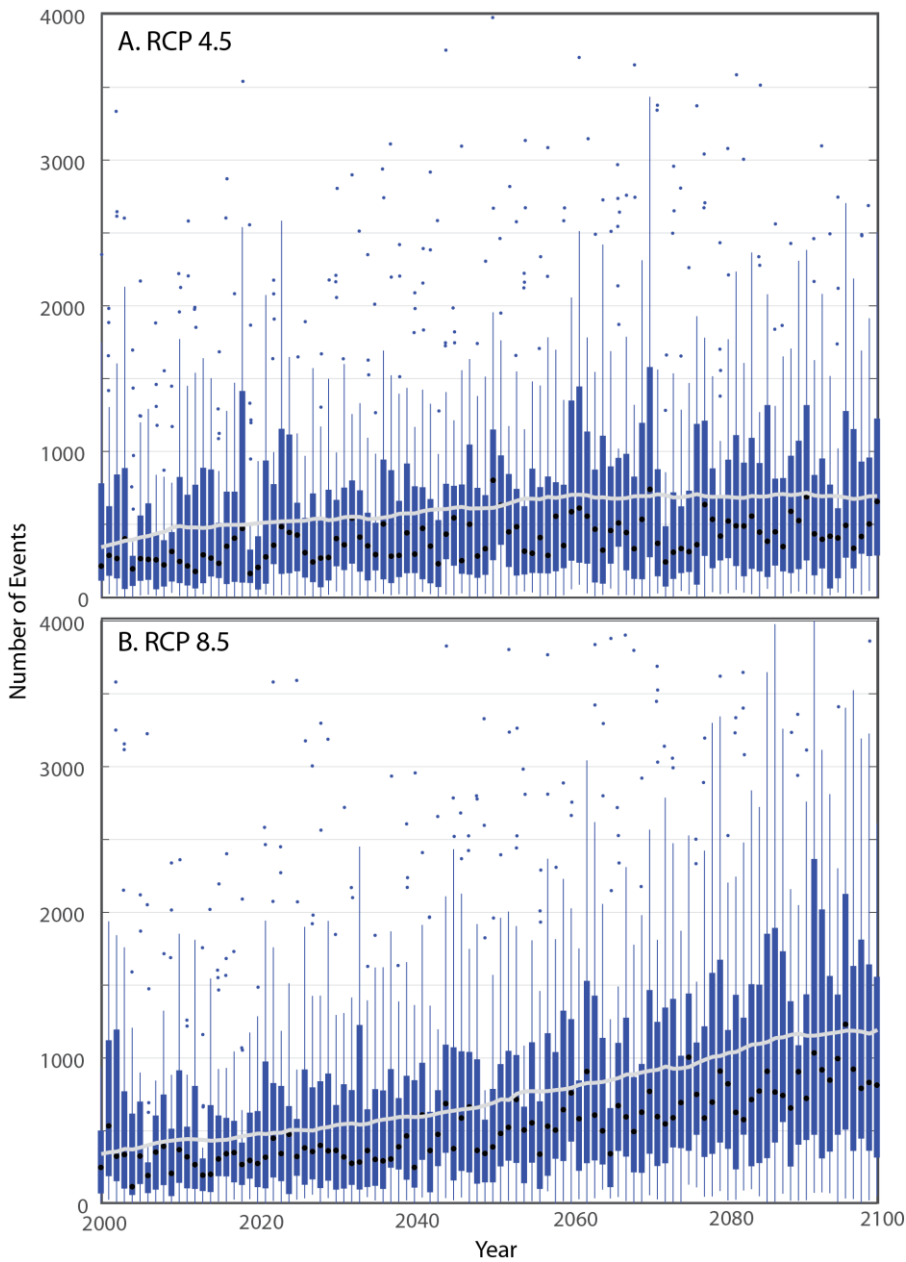
Figure 5: Number of floods throughout CONUS in each year of the 21st century, across all 29 GCMs in A) RCP4.5 and B) RCP8.5. In each plot, black dots are the median value across all 29 GCMs, thick blue bars are the middle 50% of models, whiskers extend to the 95th percentile of values, and dots represent outliers. The thick grey line is the five-year moving mean across all models. Light grey shading in background shows period used to calculate "baseline" 1% AEP event.
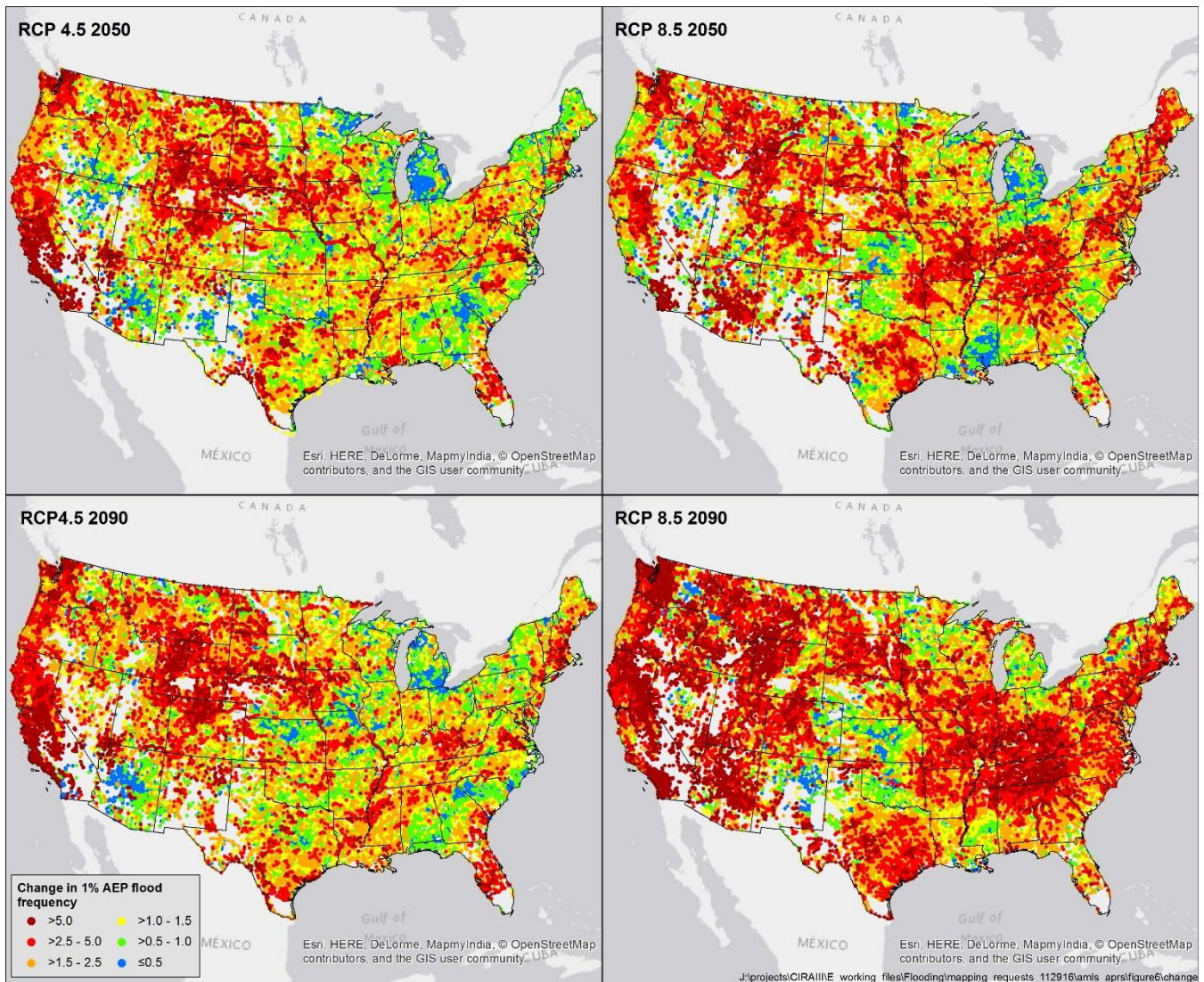
Figure 6: Change in frequency of historical 1% AEP events based on ensemble averages for specified RCP and time periods. Calculations are based on individual stream segments over 20-year periods centered on A) 2050 for RCP4.5, B) 2050 for RCP8.5, C) 2090 for RCP4.5, and D) 2090 for RCP8.5. Values are expressed as ratios (e.g., a value of 2 corresponds to a doubling in frequency of the historical 1% AEP event).
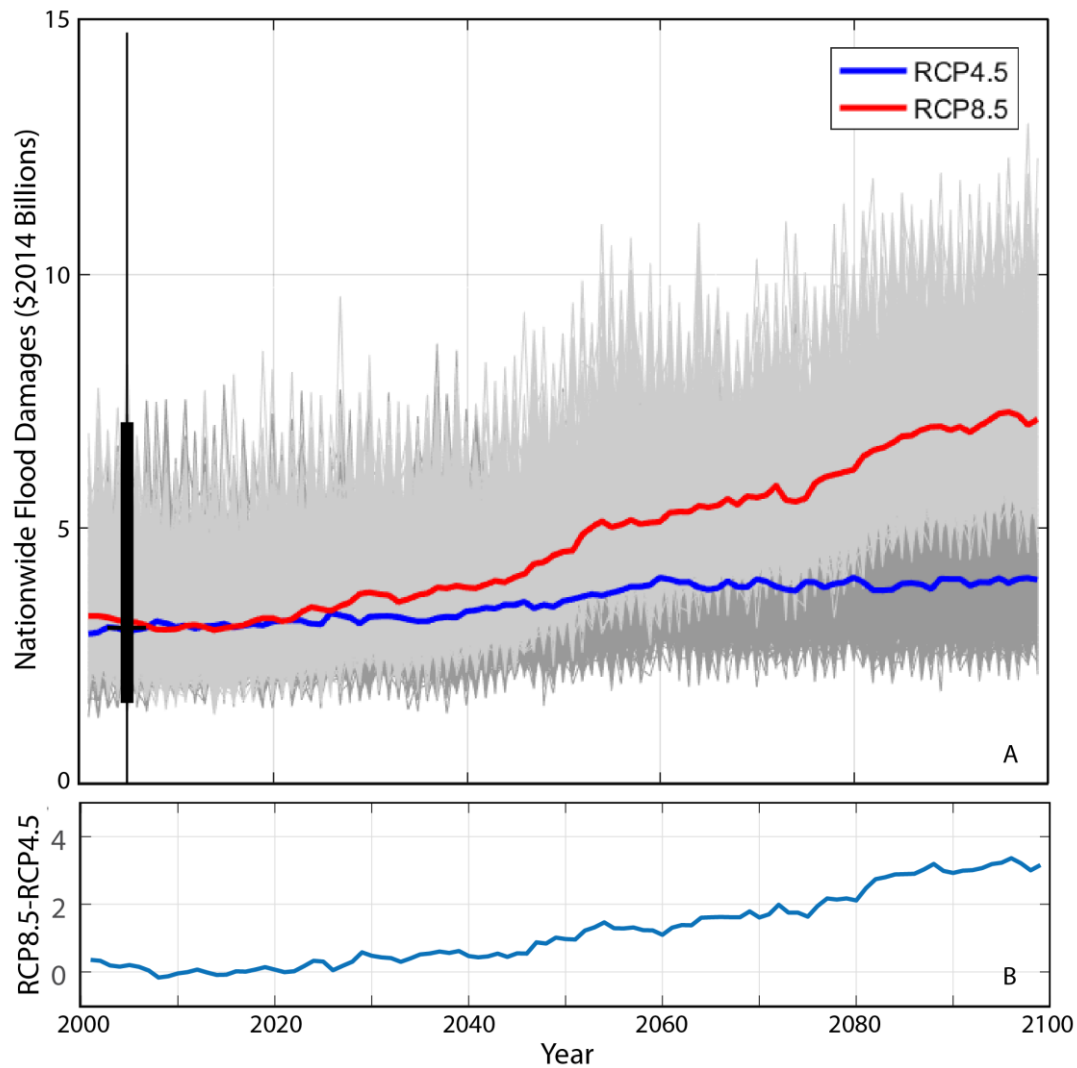
Figure 7: A) Projected national flood damages within 100-year flood zones, in 2014 dollars. Thin grey lines are 1,000 simulations of damages for RCP4.5 (dark grey) and RCP8.5 (light grey). Blue and red lines are means of simulations for the two RCPs. Box and whisker plot at left is the range of historical observed flooding in CONUS between 1903 and 2014 (10 outliers not shown). B) Difference between mean annual flood damages between RCP4.5 and RCP8.5 (billions of 2014 US dollars).
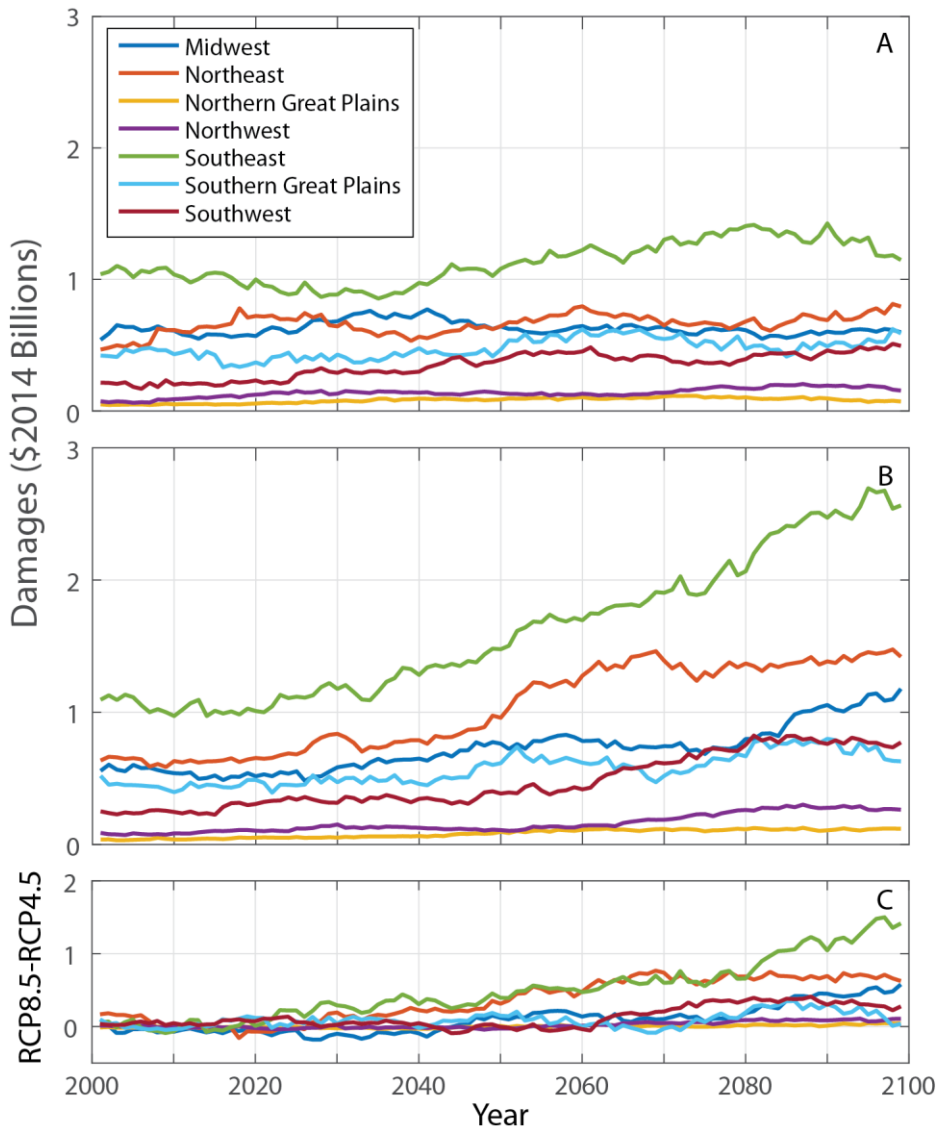
Figure 8: Average annual flooding damages by region for A) RCP4.5 and B) RCP8.5. C) Difference in annual flood damages between RCP4.5 and RCP8.5 by region (billions of 2014 US dollars). See Figure 4 for delineation of regions.